

Reaction of the Black Tea Pigment Theaflavin during Enzymatic Oxidation of Tea Catechins

Yan Li, Akane Shibahara, Yosuke Matsuo, Takashi Tanaka,* and Isao Kouno

Laboratory of Natural Product Chemistry, Graduate School of Biomedical Sciences, Nagasaki University, Bunkyo-Machi 1-14, Nagasaki 852-8521, Japan

Received October 7, 2009

Degradation of the black tea pigment theaflavin was examined in detail. Enzymatic oxidation of a mixture of epigallocatechin and epicatechin initially produced theaflavin, while prolonged reaction decreased the product. Addition of ethanol to the reaction mixture at the point when theaflavin began to decrease afforded four new products, together with theanaphthoquinone, a known oxidation product of theaflavin. The structures of the new products were determined by spectroscopic methods. One of the products was an ethanol adduct of a theanaphthoquinone precursor, and this reacted with theaflavin to give two further products. A product generated by coupling of theaflavin with epicatechin quinone was also obtained. The structures of the products indicate that oxidation and coupling with quinones are key reactions in the degradation of theaflavins. The degradation of theaflavin probably contributes to production of thearubigins.

Black tea, which is rich in polyphenols,¹ is associated with antioxidative,² anticancer,^{3,4} and anti-inflammatory^{5,6} activities. Theaflavin (**1**) and its galloyl esters⁷ are characteristic pigments found only in black tea and contribute to its color and flavor.^{8,9} The pigments are produced by oxidative condensation between catechol-type catechins [epicatechin (**2**) and its galloyl ester] and pyrogallol-type catechins [epigallocatechin (**3**) and its galloyl ester] during black tea production. However, the theaflavin content of the black tea leaf is usually 0.8–2.8% of the dried leaf depending on the fermentation conditions.^{10–13} In addition to theaflavins, numerous other oxidation products are produced, and a heterogeneous mixture of pigments with a reddish-brown color is referred to as thearubigins. Thearubigins constitute up to 60% of the solids in black tea infusions^{10,14} and are therefore very important with respect to color and taste, as well as biological activities. However, the definition of thearubigins remains ambiguous, and little is known about their chemical structures despite substantial efforts by many research groups.^{14,15} Previously, we demonstrated that theaflavins are further oxidized to give products that include dimerization products.^{16–19} In addition to the individual oxidation of **2**, **3**, and their galloyl esters,^{19–25} oxidation of theaflavins is probably involved in the formation of thearubigin components. During the enzymatic oxidation of tea catechins, a number of unstable products are produced and the subsequent decomposition of these products are key reactions in the production of thearubigins.^{22,24,25} Due to difficulties in separating the unstable intermediates by conventional chromatography, they were converted into more stable compounds in our previous study.^{24,26} During the *in vitro* oxidation study described here, we found that addition of EtOH, which was used to terminate the enzymatic reaction, affords stable EtOH adducts derived from theaflavin oxidation products. The structure of the derivatives indicated the nature of the reaction mechanisms occurring during the initial stage of theaflavin oxidation.

Results and Discussion

An aqueous solution of **2** and **3** was mixed with a Japanese pear homogenate^{18,21} and stirred vigorously at room temperature. Aliquots of the reaction mixture were mixed with EtOH to terminate the enzymatic oxidation and then analyzed by HPLC (Figure 1). The color of the reaction mixture changed from colorless to reddish-yellow in proportion to the increase in concentration of **1**. Due to the occurrence of an oxidative dimerization reaction of **3**,²⁴ the concentration of **3** decreased faster than that of **2**. When **3** was

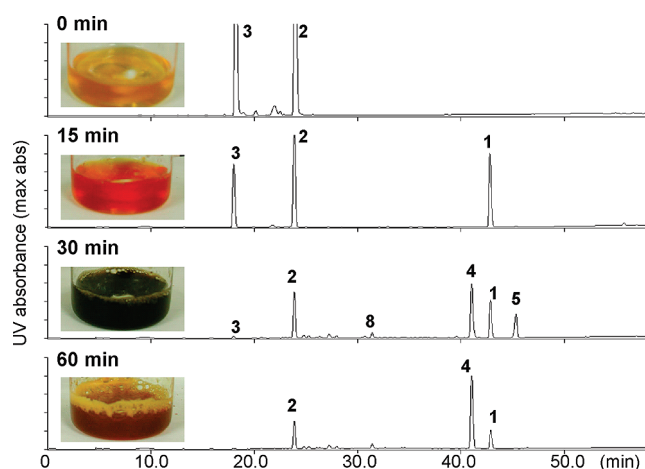


Figure 1. Color change of reaction mixture and HPLC after the reaction started. The color of the reaction mixture at 0 min was about 30 s after addition of Japanese pear homogenate. The chromatogram at 0 min was a control solution, in which water was added instead of Japanese pear homogenate.

completely consumed, the color had dramatically changed to dark green. The change in color was probably caused by the formation of a quinhydrone-type π - π complex between the benzotropolone moiety of **1** and the *ortho*-quinone unit (**2a**) derived from **2**.¹⁸ Finally, the color of the mixture became brownish-yellow. At this stage, the concentration of **1** was low and theanaphthoquinone (**4**) had accumulated.¹⁶ Interestingly, when the color had changed to dark green, the HPLC chromatogram (Figure 1C) exhibited minor peaks that were not observed at other reaction stages. To identify the unknown products, a large-scale experiment was performed and four new products, **5–8**, in addition to five known compounds, were isolated (Figure 2). The known compounds were identified as **1**, **4**, theasinensin C,²⁷ and desgalloyltheasinensins F and G.²⁸

Product **5** was detected after the reaction mixture was treated with EtOH (at 45.3 min in the HPLC, Figure 1), and this peak was not observed in the chromatogram obtained by direct analysis of the same reaction mixture without addition of EtOH. The product was obtained as a brown, amorphous powder that showed UV maxima at 257 and 348 nm. The MALDITOFMS spectrum showed the $[M + Na]^+$ peak at m/z 613. The appearance of 31 signals in the ¹³C NMR spectrum and the results of elemental analysis suggested that the molecular formula is C₃₁H₂₆O₁₂. Among the carbon signals (Table 1), 18 signals were assigned to the A- and

* To whom correspondence should be addressed. Tel: 81-95-819-2433. Fax: 81-95-819-2477. E-mail: t-tanaka@nagasaki-u.ac.jp.

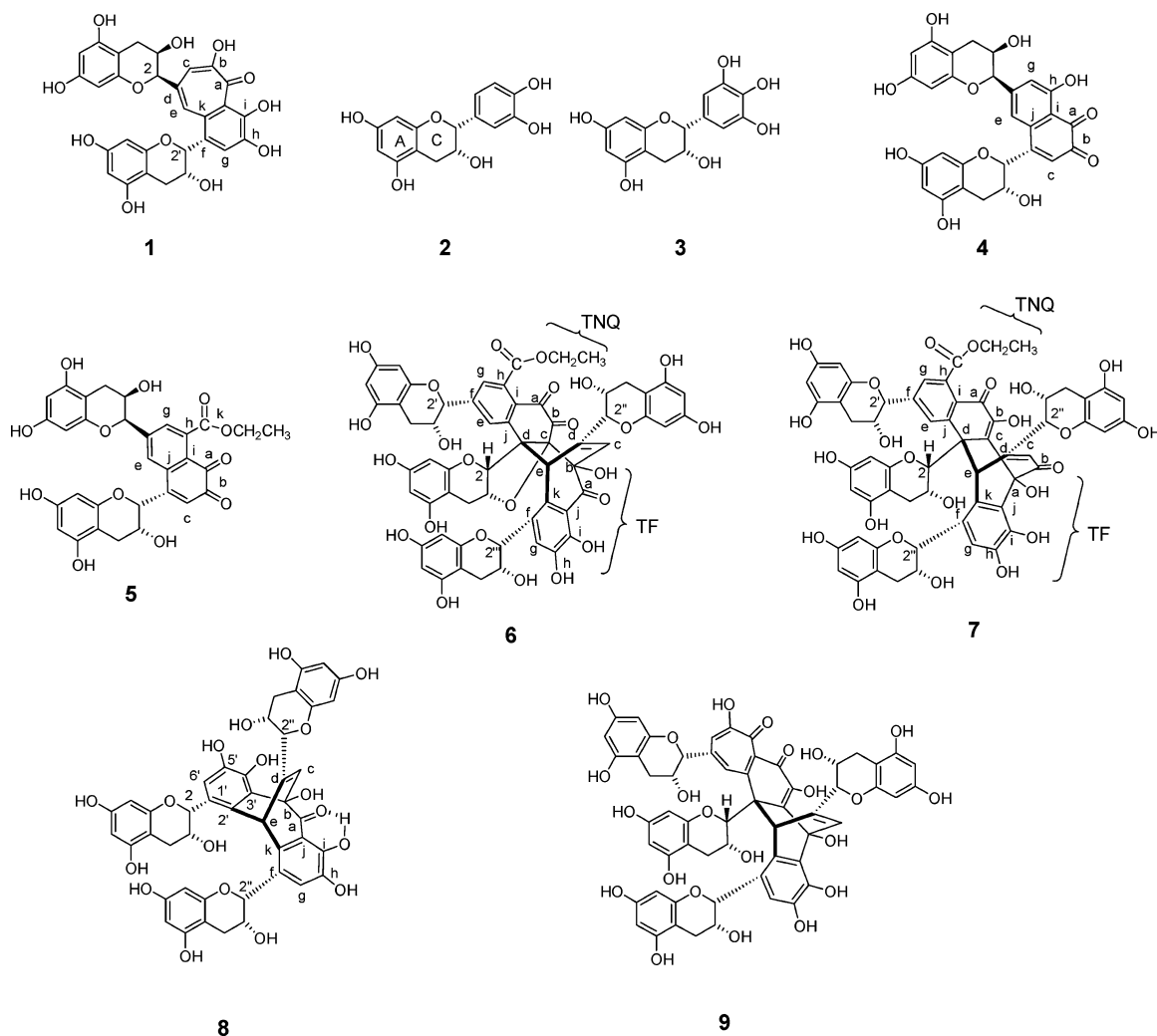


Figure 2. Structures of compounds 1–8.

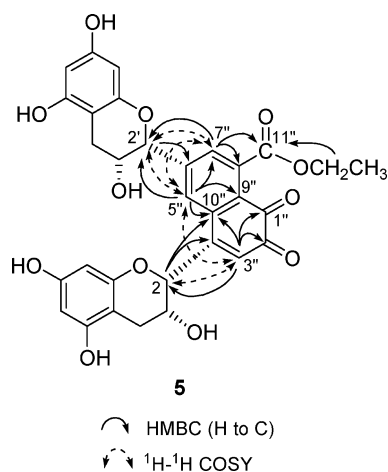


Figure 3. Selected HMBC and ^1H – ^1H COSY correlations for compound 5.

C-rings of the flavan-3-ol skeleton and two (δ 62.2 and 14.2) were attributed to the ethyl group on the basis of HSQC and HMBC experiments. The remaining 11 signals were related to the theanaphthoquinone moiety of **4**, except for an additional carboxylic carbon at δ 169.4 (C-k). In the HMBC spectrum, two conjugated carbonyl carbons [δ 179.7 (C-a), 180.9 (C-b)] were correlated with an aromatic proton at δ 6.85 (H-c), which also correlated with C-2 (C-ring) (δ 75.5). In addition, long-range allylic coupling between

H-2 and H-c was observed in the ^1H – ^1H COSY spectrum, indicating the presence of the same partial structure as that of **4**. In turn, both H-2 and H-c showed long-range ^1H – ^1H coupling with an aromatic proton, H-e, and H-e was correlated with the remaining aromatic proton H-g and with H-2' of another C-ring. Furthermore, H-g showed HMBC correlation with an additional carboxylic carbon, C-k, which also correlated with the methylene protons of the ethyl group. These spectroscopic observations allowed us to construct the structure of this product as given in formula **5**. The HMBC correlations illustrated in Figure 3 supported the structure. This product was formed by addition of EtOH to a carbonyl group of theaflavin quinone (**1a**) and subsequent rearrangement (Scheme 1). The intermediate **1a** was also presumed to be a precursor of **4**. Isolation of **5** in this experiment evidenced generation of **1a** and **4a**.

Product **6** showed an $[\text{M} + \text{H}]^+$ peak at 1153 and an $[\text{M} + \text{Na}]^+$ peak at m/z 1175, indicating that this product is a tetrameric catechin. The ^1H and ^{13}C NMR spectra (Table 2) showed four sets of signals due to flavan A- and C-rings. In addition, signals attributable to two aromatic rings, an ethoxy group, three carbonyl carbons, one carboxylic carbon, one double bond, three aliphatic quaternary carbons, and an aliphatic methine were observed. In the HMBC spectrum (Figure 4), correlations of the C-ring H-2''' and aromatic proton TF-g-H indicated a catechol-type aromatic ring (TF-f–TF-k). A phenolic hydroxy proton resonating at δ 11.79 was correlated with aromatic carbons TF-h, i, and j; thus, this proton was assigned as TF-i-OH, and the chemical shift indicated hydrogen bonding with a carbonyl group (TF-a) attached to TF-j. The TF-j

Table 1. ^1H and ^{13}C NMR Data for Theanaphthoquinone (**4**) and Compound **5** (in acetone- d_6)

position	theanaphthoquinone (4)		5	
	^1H	^{13}C	^1H	^{13}C
2	5.38, br s	75.4	5.48, s	75.5
3	4.39, br d (2.7)	64.8	4.46, m	64.1
4	2.96, dd (4.6, 16.5)	28.9	2.98, br d (16.5)	28.7
	2.82, br d (16.5)		2.84, br d (16.5)	
4a		99.7		99.7
5		157.7 ^{a,b}		157.8 ^a
6	6.06, d, (2.3)	96.7 ^b	6.07, d (2.3)	96.7 ^b
7		157.6 ^a		157.6 ^a
8	6.00, d (2.3)	95.6 ^b	6.07, d (2.3)	95.7 ^b
8a		156.2		156.1
2'	5.16, br s	78.9	5.26, s	78.8
3'	4.43, m	66.3	4.43, m	66.3
4'	2.71, dd (3.7, 16.6)	28.8	2.92, dd (4.6, 16.7)	28.8
	2.89, dd (4.6, 16.6)		2.75, dd (3.2, 16.7)	
4a'		99.4		99.3
5'		157.5 ^a		157.6 ^a
6'	6.06, d (2.3)	96.7 ^b	6.05, s	96.7 ^b
7'		157.6 ^a		157.6 ^a
8'	6.00, d (2.3)	95.6 ^b	6.03, s	95.7 ^b
8a'		156.1		156.1
a		180.6		179.7
b		183.4		180.9
c	6.79, d (1.0)	126.9	6.85, d, 1.0	127.5
d		152.2		152.6
e	7.33, d (1.0)	118.1	7.98, d, 1.0	125.8
f		152.9		148.9
g	7.44, d (1.0)	120.1	7.72, d, 1.0	128.1
h		166.9		138.3
i		115.2		128.6
j		133.9		134.5
k				169.4
OCH ₂			4.40, 2H, m	62.2
CH ₃			1.35, 3H, t, 7.1	14.2

^{a,b} Assignments may be interchanged in each column.

and TF-k carbons showed correlations with the methine proton TF-e (δ 6.06), and, in turn, the TF-e proton correlated to double-bond carbons (TF-c and TF-d) and an oxygen-bearing quaternary carbon (TF-b). The olefinic proton TF-c was correlated to the C-ring C-2''. ^1H - ^1H long-range coupling between the olefinic protons TF-c and H-2'' was also observed in the ^1H - ^1H COSY spectrum. Furthermore, a hydroxy group (δ 6.44), assignable to TF-b-OH, showed correlations to TF-a and TF-b. These observations suggest the presence of a theaflavin unit in which TF-b and TF-e carbons are connected to the remaining structural component. The TF-b-OH also showed an HMBC cross-peak with an oxygen-bearing quaternary carbon TNQ-c (δ 98.1), and a TF-e methine proton was correlated to the TNQ-d carbon. The TNQ-d carbon also showed a correlation peak with an aromatic proton, TNQ-e. The aromatic ring (TNQ-e-TNQ-j) was attached to the C-ring C-2', because the

aromatic protons TNQ-e and TNQ-g showed HMBC correlations to C-2'. In addition, correlation peaks of the ester carbonyl carbon (δ 170.3), the methylene protons of the ethoxy group, and the aromatic proton at TNQ-g were similar to those observed for **5**. The location of the remaining two conjugated carbonyl carbons at δ 187.8 (TNQ-a) and 198.0 (TNQ-b) was concluded to be between TNQ-i and TNQ-c, because this TNQ unit was suggested to originate from compound **5**. From these spectroscopic observations and the molecular weight evidenced by HRFABMS, the molecular formula of **6** was deduced to be $\text{C}_{60}\text{H}_{48}\text{O}_{24}$, which indicates that the degree of unsaturation was 37. This implies that an ether ring was formed between the oxygen-bearing quaternary carbon TNQ-c and the C-ring C-3 (δ 70.1) hydroxy group. C-3 (δ 70.1) resonated at a much lower field than the other C-ring C-3 carbons ($\Delta\delta > +4.0$). In addition, an accompanying upfield shift of C-4 (δ 24.3) also supported the conclusion of ether ring formation.

The stereochemistry was determined by a NOESY experiment; the methine proton TF-e showed a NOE with H-2, H-2'', and TNQ-e. H-2''' was correlated with H-2''. Furthermore, the C-ring H-3' exhibited a correlation peak with A-ring H-8 and H-8''. These NOESY correlations and molecular modeling indicated that the configuration at TF-e and TNQ-d could be concluded to be as shown in formula **6**. The possible mechanism of formation **6** is illustrated in Scheme 2, in which initial attack of the benzotropolone of **1** to the enone of **5** is followed by ring formation between TNQ-c and TF-b (route A) and subsequent Michael addition of C-3-OH to TNQ-c.

The ^1H and ^{13}C NMR spectra of compound **7** resembled those of **6** (Table 2), and the FABMS data exhibited an $[\text{M} + \text{H}]^+$ peak at m/z 1155, indicating that the molecular weight of **7** was 2 mass units larger than that of **6**. The HMBC correlations of **7** (Figure 4) revealed the presence of partial structures similar to those of **6**. C-2' of one of the four sets of flavan-A- and C-rings is attached to an aromatic ring bearing an ethoxycarbonyl group of the TNQ subunit. C-2 of a second A/C-ring showed a HMBC correlation with a quaternary carbon (TNQ-d), which further correlated with the aromatic proton of TNQ-e and an aliphatic methine proton of TF-e. Chemical shifts of C-3 and C-4 of this C-ring resonated at higher and lower fields, respectively, compared with those of **6**, indicating the absence of the additional etherocyclic linkage in **6**. C-2'' and C-2''' of the remaining two sets of A/C-rings are connected to C-d and C-f of the TF subunit. The connection between the TNQ and TF subunits was shown to be similar to that of **6** by observation of similar HMBC correlations of H-e in the TF subunit. One of the remarkable differences between **7** and **6** was the presence of an enolic group, which showed correlation peaks with the methine proton of TF-e and H-2 through 3J (C-c) and 4J (C-b) correlations. This enolic group was assigned to C-b and C-c of the TNQ subunit. Another difference was observed in the TF subunit: the ^{13}C NMR chemical shift of TF-i of **7** (δ 144.7) was observed

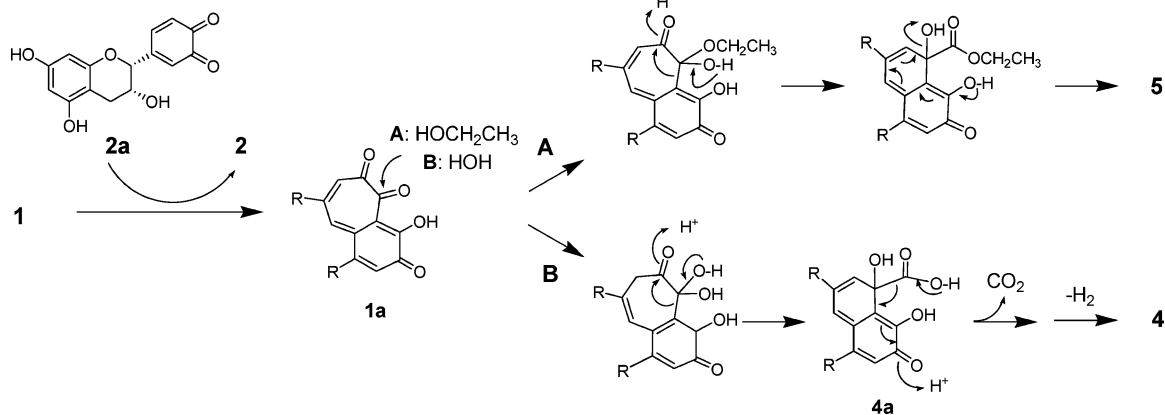
Scheme 1. Proposed Mechanism for Formation of **4** and **5** from **1**

Table 2. ^{13}C and ^1H NMR Data for **6** and **7** (in acetone- d_6)

atom no.	6		7	
	^{13}C	^1H	^{13}C	^1H
	TNQ unit			
2	76.0	4.94, d (2.5)	81.4	3.99, br s
3	70.1	4.47, m	62.8	3.99, br s
4	24.3	2.79, dd (1.9, 17.4) 2.60, dd (5.0, 17.4)	31.5	2.37, dd (4.2, 16.7) 2.46, br d (16.7)
4a	88.0		99.0	
5	157.9 ^a		157.3 ^a	
6	96.5	5.80, d (2.3)	95.6	5.97, d (2.3)
7	157.7 ^a		157.6 ^a	
8	96.1	5.70, d (2.3)	96.1	5.97, d (2.3)
8a	155.0 ^a		156.0 ^a	
2'	78.4	5.15, br s	78.6	5.03, br s
3'	65.9	4.82, br s	66.6	4.39, br s
4'	29.2	2.89, 2H, br s	28.0	2.56, dd (3.6, 16.3) 2.84, m
4a'	99.8		99.5	
5'	157.6 ^a		157.4 ^a	
6'	96.6 ^b	6.04, d (2.3) ^c	96.4 ^b	5.91, d (2.3) ^c
7'	157.3 ^a		157.5 ^a	
8'	96.0 ^b	5.91, d (2.3) ^c	96.5 ^b	5.93, d (2.3) ^c
8a'	155.0 ^a		156.3 ^a	
TNQ-a	187.8		180.3	
TNQ-b	198.0		143.0	
TNQ-c	98.1		125.1	
TNQ-d	55.2		50.9	
TNQ-e	129.0	8.24, s	129.2	8.56, s
TNQ-f	145.5		144.5	
TNQ-g	125.8	7.62, s	125.9	7.53, s
TNQ-h	136.9		135.1	
TNQ-i	126.8		128.5	
TNQ-j	141.7		149.5	
COO	170.3		170.4	
CH ₂	61.6	4.22, 2H, m	61.8	4.30, 2H, q (7.1)
CH ₃	14.2	1.24, 3H, t (7.1)	14.3	1.37, 3H, t (7.1)
	TF unit			
2''	76.0	4.80, br s	80.4	4.08, br s
3''	65.6	4.49, br s	62.7	3.77, br s
4''	28.0	2.74, dd (4.4, 16.0) 2.27, dd (6.2, 16.0)	29.2	2.65, 2H, m
4a''	99.2		99.4	
5''	157.6 ^a		157.4 ^a	
6''	95.0 ^b	5.67, d (2.3)	96.8 ^b	6.09, d (2.3)
7''	157.3 ^a		157.5 ^a	
8''	96.6 ^b	5.88, d (2.3)	95.6 ^b	6.03, d (2.3)
8a''	156.3 ^a		156.7 ^a	
2'''	76.0	5.63, br s	75.4	5.89, br s
3'''	63.3	4.88, br s	65.7	4.38, br s
4'''	31.0	3.08, dd (4.1, 16.7) 2.97, br d (16.7)	31.0	2.89, m 2.90
4a'''	100.5		100.1	
5'''	157.3 ^a		157.5 ^a	
6'''	97.4	6.25, d (2.3)	95.6	6.03, d, (2.3)
7'''	157.1 ^a		157.6 ^a	
8'''	96.8	6.42, d (2.3)	97.0	6.08, d, (2.3)
8a'''	156.4 ^a		157.1 ^a	
TF-a	186.3		86.3	
TF-b	65.7		189.4	
TF-c	123.6	5.75, d (1.6)	126.9	6.21, br s
TF-d	165.8		159.3	
TF-e	41.5	6.06, br s	44.7	6.03, br s
TF-f	129.9		129.8	
TF-g	125.2	7.86, s	116.4	7.19, s
TF-h	146.8		145.5	
TF-i	153.2		144.7	
TF-j	116.2		113.9	
TF-k	132.6		127.4	
TF-b-OH		6.44, s		
TF-i-OH		11.79, s		

^{a-c} Assignments may be interchanged in each column.

at a higher field than that of **6** (δ 153.2). This suggests that this aromatic ring was not conjugated with a carbonyl group, and thus, the oxygen-bearing quaternary carbon at δ 86.3 was attributed to C-a. Accordingly, a conjugated carbonyl carbon at δ 189.4 was

assigned to C-b in the TF unit and C-a was connected to C-c of the TNQ subunit. Compound **7** gradually decomposed during NMR experiments to give a mixture of decomposition products. In the spectra of the mixture, a set of ^1H NMR peaks coincided with those of compound **6**. The mechanism of formation of **6** from **1** and **7** was deduced to be route B in Scheme 2. The compound **7** is related to bistheafavin B (**9**), previously reported as an oxidation product of **1**.¹⁷

In contrast to the above three products, the ^1H and ^{13}C NMR spectra of **8** (Table 3) did not show signals of the ethyl group; thus **8** was not an ethanol adduct of reaction products. This product was detected by HPLC when **1** began to oxidize (Figure 1). The MALDITOFMS of **8** showed an $[\text{M} + \text{Na}]^+$ peak at m/z 875, indicating this product is a flavan-3-ol trimer. The HMBC spectrum revealed the presence of a TF subunit similar to that of **6** (Figure 5). The chemical shift (δ 12.91) of the phenolic hydroxy proton connected to TF-i showed hydrogen bonding with the TF-a carbonyl group. In addition, the HMBC correlations of the C-ring H-2''' and the aromatic proton H-6''' indicate the presence of an epicatechin subunit. The connection between these subunits was obvious from the HMBC correlation of H-e to C-1''', C-2''', and C-3''', and H-c to C-3''' (Figure 5). The NOESY spectrum showed correlations between H-e and all three C-ring H-2 protons. However, this observation is not sufficient to determine the configuration at C-e and C-b. Thus, the structure of **8** was tentatively presumed to have the same configuration as that of **6**. A possible mechanism to explain the genesis of **8** is illustrated in Scheme 3. Compound **8** represents the condensation product of **1** and epicatechin quinone (**2a**).

The results indicate that oxidation and coupling with quinones are key reactions in the degradation of theaflavins. Our previous study suggested that epicatechin quinone (**2a**) was first generated in the reaction mixture because of higher enzyme specificity to **2**. Subsequently, **2a** reacts with **3** to yield **1**.^{10,18} The quinone **2a** acts as an oxidant and first oxidizes **3** due to the low redox potential of **3**. The resulting quinone of **3** was used for producing theasinensins,²⁰ therefore, the concentration of **3** decreased faster than **2**. The oxidation of **1** to theanaphthoquinone (**4**) by **2a** began when **3** was depleted (Scheme 1), and this reaction is the major route for degradation of **1**. The formation of **5** supported this reaction mechanism. In addition to oxidation, our results demonstrated that addition of the benzotropolone ring to the quinones occurs during decomposition of **1** (Schemes 2 and 3). The final product **4** of this experiment has not previously been found in black tea. Probably, **4** undergoes further coupling reactions with coexisting compounds. It is evidenced by the production of **9** and related compounds, **6** and **7**, isolated in this study. The major part of the black tea polyphenols, including thearubigins, still remained to be identified.¹⁴ The results of the present study indicate the reaction mechanism for theaflavin decomposition, which probably participates in the production of the unknown products.

Experimental Section

General Experimental Procedures. IR and UV spectra were obtained using JASCO FT/IR-410 and JASCO V-560 spectrophotometers, and optical rotations were measured using a JASCO DIP-370 digital polarimeter (JASCO Co., Tokyo, Japan). Elemental analysis was conducted with a Perkin-Elmer 2400 α analyzer (Perkin-Elmer Inc., Waltham, MA). ^1H and ^{13}C NMR, ^1H - ^1H COSY, NOESY, HSQC, and HMBC spectra were recorded in a mixture of acetone- d_6 and D_2O , using a Varian Unity plus 500 spectrometer operating at 500 MHz for ^1H and 125 MHz for ^{13}C (Varian, Palo Alto, CA). Coupling constants are expressed in Hz, and chemical shifts are given on a δ (ppm) scale. HMQC, HMBC, and NOESY experiments were performed using standard Varian pulse sequences. FAB and HR-FABMS data were recorded on a JEOL JMS-700N spectrometer (JEOL Ltd., Tokyo, Japan) with glycerol or *m*-nitrobenzyl alcohol matrixes. MALDITOFMS data were recorded on a Voyager-DE Pro spectrometer (Applied Biosystems, Foster City, CA), and 2,5-dihydroxybenzoic acid (10 mg/mL in 50%

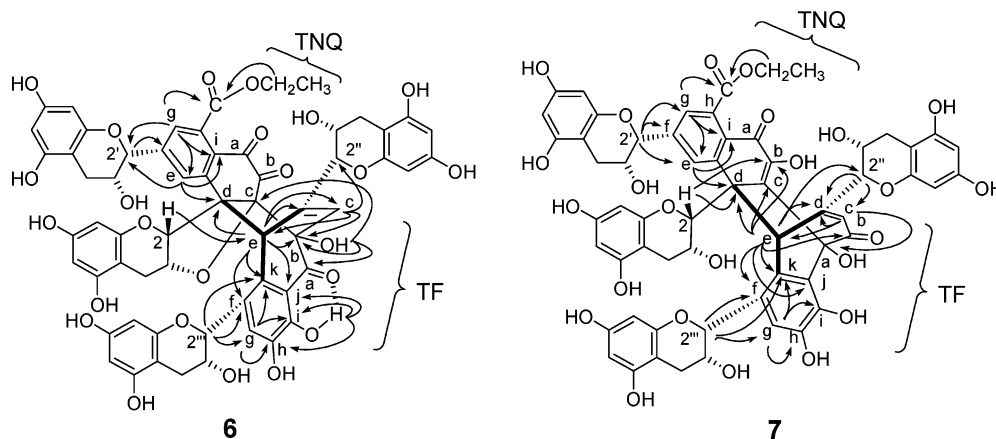


Figure 4. Selected HMBC correlations for **6** and **7**.

Scheme 2. Proposed Mechanism for Formation of **6** and **7**

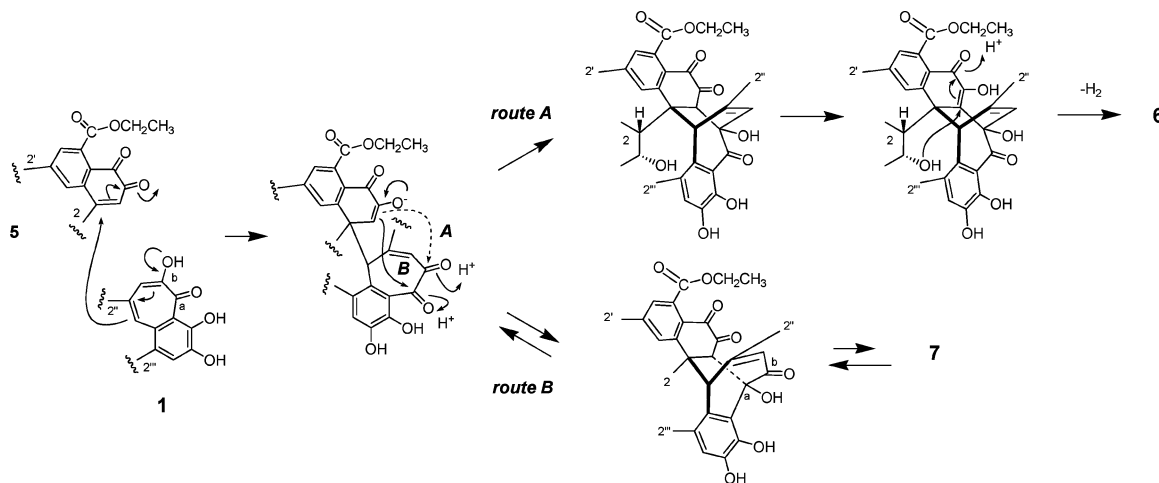


Table 3. ^{13}C and ^1H NMR Data for **8** (in acetone- d_6)

position	^{13}C	^1H	position	^{13}C	^1H
2	75.8	5.38, br s	8	96.1 ^c	6.01, d, (1.6)
3	64.8	3.98, br s	8a	155.8	
4	29.9	2.61, dd (4.0, 16.7)	2'	75.0	5.68, br s
		2.67, dd (16.7)	3'	67.0	4.27, br s
4a	99.7 ^a		4'	29.3	2.82, br d (16.5)
5	157.3 ^b				3.06, dd (4.4, 16.5)
6	96.1 ^c	5.87, d (1.6)	4a'	99.1	
7	157.0 ^b		5'	157.6 ^b	
8	95.3 ^c	5.86, d (1.6)	6'	96.0 ^c	6.00, d (1.6)
8a	155.0 ^b		7'	157.5 ^b	
1'	128.1		8'	95.3 ^c	5.94, d (1.6)
2'	130.0		8a'	156.9 ^b	
3'	121.7		a	197.8	
4'	143.7 ^d		b	85.2	
5'	144.4 ^d		c	132.8	6.43, s
6'	116.2	7.19, s	d	146.8	
2''	77.2	4.94, br s	e	41.4	5.80, br s
3''	65.1	4.60, br s	f	127.8	
4''	28.3	2.43, dd (6.5, 15.8)	g	123.3	7.51, d (1.0)
		2.79, dd (4.7, 15.8)	h	145.6	
4a''	99.8 ^a		i	155.4	
5''	157.8 ^b		j	113.3	
6''	96.4 ^c	6.02, d (1.6)	k	134.0	
7''	157.7 ^b		C-i-OH	12.91, s	

^{a-d} Assignments may be interchanged.

acetone containing 0.05% TFA) was used as the matrix. Column chromatography was performed using Sephadex LH-20 (25–100 μm , GE Healthcare Bio-Sciences AB, Uppsala, Sweden), Diaion HP20SS (Mitsubishi Chemical, Tokyo, Japan), Bondapak C₁₈ 125A (37–35 μm , Waters Co., Milford, MA), and Chromatorex ODS (100–200 mesh; Fuji Silysia Chemical, Kasugai, Japan) columns.

TLC was performed on 0.2 mm thick precoated Kieselgel 60 F₂₅₄ plates (Merck, Darmstadt, Germany) using toluene–ethyl formate–formic acid (1:7:1, v/v). Spots were detected by UV illumination, sprayed with 2% methanolic FeCl₃ or 10% H₂SO₄ reagent, and then heated. Analytical reversed-phase HPLC was performed on a Cosmosil 5C₁₈-AR II column (Nacalai Tesque Inc., Tokyo, Japan; 4.6 mm i.d. \times 250 mm) using an elution gradient of 4–30% (39 min) and 30–75% (15 min) CH₃CN in 50 mM H₃PO₄ (flow rate 0.8 mL/min; detection using a JASCO MD-910 photodiode array detector). Preparative HPLC was performed on a Cosmosil 5C₁₈-AR-II column (Nacalai Tesque Inc.; 10 mm i.d. \times 250 mm) using a linear elution gradient of 20–70% CH₃CN in 0.5% TFA. Japanese pear was purchased at a local market, and epicatechin (**2**) and

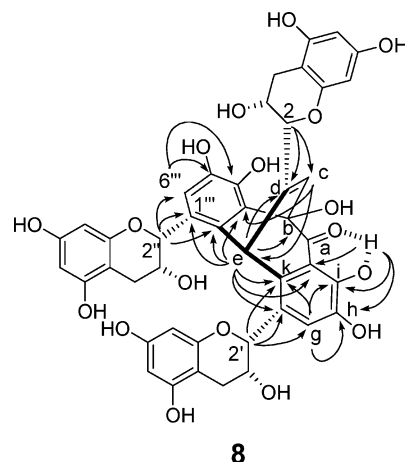
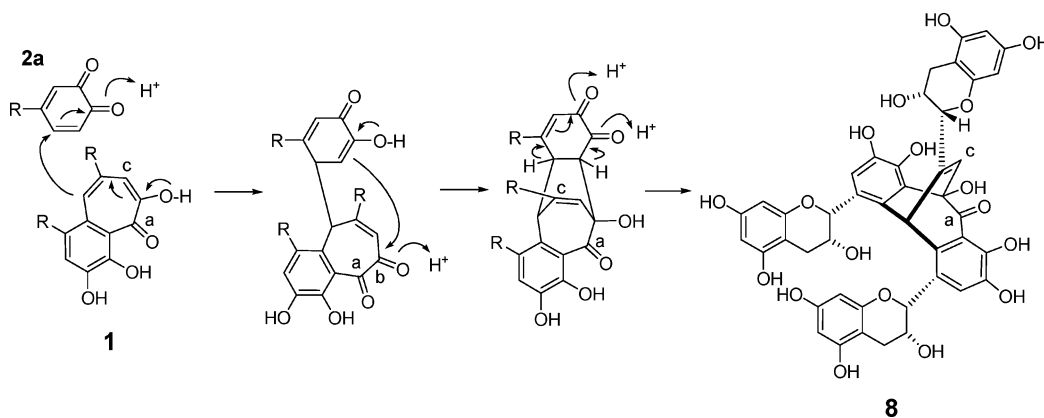


Figure 5. Selected HMBC correlations for **8**.

Scheme 3. Proposed Mechanism for Formation of **8**

epigallocatechin (**3**) were extracted and separated from commercial green tea and purified by crystallization from H₂O.

Enzymatic Oxidation of 2 and 3. Japanese pear (100 g) was homogenized in H₂O (100 mL) and filtered through four layers of gauze. The homogenate (20 mL) was mixed with an aqueous solution (5 mL) of **2** (50 mg) and **3** (50 mg) and vigorously stirred at room temperature. Aliquots (1.0 mL) of the mixture were taken at 15, 30, and 60 min after addition of the homogenate, mixed with EtOH (3 mL), and analyzed by HPLC. A solution of **2** (10 mg) and **3** (10 mg) in 75% EtOH (20 mL) was used for the control solution.

Large-Scale Enzymatic Oxidation of 2 and 3. Japanese pear (500 g) was homogenized in H₂O (500 mL) and filtered through four layers of gauze. The homogenate (1000 mL) was mixed with an aqueous solution (300 mL) of **2** (2.0 g) and **3** (2.0 g) and vigorously stirred for 30 min at room temperature. The mixture was poured into EtOH (3 L) and gently stirred for 30 min, and insoluble material was removed by filtration. The filtrate was concentrated by evaporation until the EtOH was completely removed. The resulting aqueous solution was subjected to Diaion HP20SS column chromatography (4.0 cm i.d. × 26 cm) using H₂O containing an increasing proportion of MeOH (10% stepwise elution from 0% to 100%, each 300 mL). The eluate was monitored by TLC and separated into 11 fractions. The first fraction mainly contained sugars and was not examined further. Fractions 2 (103 mg), 3 (59 mg), and 4 (173 mg) were separately subjected to Sephadex LH-20 column chromatography (40–60% MeOH) to give theasinensin C (45 mg from Fr. 2) and desgalloyl theasinensins F (31 mg, from Fr. 3) and G (80 mg, from Fr. 4). Fraction 7 (722 mg) was successively separated by Sephadex LH-20 (60% MeOH) and preparative HPLC using Cosmosil 5C₁₈ AR II to yield product **8** (11.0 mg). Fraction 8 (358 mg) was applied to a column of Chromatorex ODS (30–100% MeOH) and then Bondapak C₁₈ (20–60% MeOH) to yield products **6** (62 mg) and **7** (48 mg). Fraction 10 (1.6 g) was subjected to Sephadex LH-20 column chromatography (80–100% MeOH) to afford **4** (448 mg) and **1** (953 mg). Fraction 11 (571 mg) was separated by Sephadex LH-20 column chromatography (80–100% MeOH) to yield product **5** (206 mg).

Product 5: brown, amorphous powder; $[\alpha]_D^{29}$ -276 (*c* 0.06, MeOH); MALDITOFMS *m/z* 613 [M + Na]⁺; UV (EtOH) λ_{\max} nm (log ϵ) 257 (4.34), 348 (4.86); IR ν_{\max} cm⁻¹ 3389, 1694, 1613, 1516, 1467; *anal.* C 60.53%, H 4.80%, calcd for C₃₁H₂₆O₁₂·1.5H₂O, C 60.29%, H 4.73%; ¹H NMR (500 MHz, acetone-*d*₆) and ¹³C NMR (125 MHz, acetone-*d*₆) data, see Table 1.

Product 6: brown, amorphous powder; $[\alpha]_D^{29}$ $+295$ (*c* 0.06, MeOH); FABMS *m/z* 1153 [M + H]⁺, 1175 [M + Na]⁺; UV (EtOH) λ_{\max} (log ϵ) nm 270 (4.23), 377 (3.67); IR ν_{\max} cm⁻¹ 3389, 1697, 1632, 1517, 1467; HR-FABMS *m/z* 1153.2726 [M + H]⁺ (calcd for C₆₀H₄₈O₂₄; 1153.2712); ¹H NMR (500 MHz, acetone-*d*₆) and ¹³C NMR (125 MHz, acetone-*d*₆) data, see Table 2.

Product 7: brown, amorphous powder; $[\alpha]_D^{18}$ -36 (*c* 0.05, MeOH); FABMS *m/z* 1155 [M + H]⁺; UV (EtOH) λ_{\max} nm (log ϵ) 272 (4.07), 378 (4.61); IR ν_{\max} cm⁻¹ 3372, 1710, 1675, 1666; *anal.* C 58.82%, H 4.84%, calcd for C₆₀H₅₀O₂₄·4H₂O, C 58.73%, H 4.76%; ¹H NMR (500 MHz, acetone-*d*₆) and ¹³C NMR (125 MHz, acetone-*d*₆) data, see Table 6.

Product 8: brown, amorphous powder; $[\alpha]_D^{18}$ $+50$ (*c* 0.05, MeOH); MALDITOFMS *m/z* 875 [M + Na]⁺; UV (EtOH) λ_{\max} nm (log ϵ) 212

(5.32), 272 (4.07); IR ν_{\max} cm⁻¹ 3353, 1631, 1607, 1513, 1506; *anal.* C 59.85%, H 4.98%, calcd for C₄₄H₃₆O₁₈·2H₂O, C 59.46%, H 4.54%; ¹H NMR (500 MHz, acetone-*d*₆) and ¹³C NMR (125 MHz, acetone-*d*₆) data, see Table 3.

Acknowledgment. The authors are grateful to Mr. K. Inada and Mr. N. Yamaguchi for NMR and MS measurements. This work was supported by a Grant-in-aid for Scientific Research No. 18510189 from the Japan Society for the Promotion of Science.

Supporting Information Available: ¹H and ¹³C NMR spectra for products **5–8**; ¹H–¹H COSY, HSQC, and HMBC spectra of **5**, **6**, and **8**; and NOESY spectrum of **6**. This material is available free of charge via the Internet at <http://pubs.acs.org>.

References and Notes

- (1) Shahidi, F.; Naczki M. *Phenolics in Food and Nutraceuticals*; CRC Press: Boca Raton, 2004; pp 241–312.
- (2) Luczaj, W.; Skrzydlewska, E. *Prev. Med.* **2005**, *40*, 910–918.
- (3) Way, T.-Z.; Lee, H.-H.; Kao, M.-C.; Lin, J.-K. *Eur. J. Cancer* **2004**, *40*, 2165–2174.
- (4) Krishnan, R.; Maru, G. B. *J. Agric. Food Chem.* **2004**, *52*, 4261–4269.
- (5) Maity, S.; Ukil, A.; Karmakar, A.; Datta, N.; Chaudhuri, T.; Veda-siromoni, J. R.; Ganguly, D. K.; Das, P. K. *Eur. J. Pharmacol.* **2003**, *470*, 103–112.
- (6) Sang, S.; Lambert, J. D.; Tian, S.; Hong, J.; Hou, Z.; Ryu, J.-H.; Stark, R. E.; Rosen, R. T.; Huang, M.-T.; Yang, C. S.; Ho, C.-T. *Bioorg. Med. Chem.* **2004**, *12*, 459–467.
- (7) Takino, Y.; Imagawa, H.; Horikawa, H.; Tanaka, A. *Agric. Biol. Chem.* **1964**, *28*, 64–71.
- (8) Hashimoto, F.; Nonaka, G.; Nishioka, I. *Chem. Pharm. Bull.* **1992**, *40*, 1383–1389.
- (9) Wang, D.; Kurasawa, E.; Yamaguchi, Y.; Kubota, K.; Kobayashi, A. *J. Agric. Food Chem.* **2001**, *49*, 1900–1903.
- (10) Haslam, E. *Practical Polyphenolics, From Structure to Molecular Recognition and Physiological Action*; Cambridge University Press, 1998; pp 335–373.
- (11) Hall, M. N.; Robertson, A.; Scotter, C. N. G. *Food Chem.* **1988**, *80*, 283–290.
- (12) Sakakibara, H.; Honda, Y.; Nakagawa, S.; Ashida, H.; Kanazawa, K. *J. Agric. Food Chem.* **2003**, *51*, 571–581.
- (13) Liang, Y.; Lu, J.; Zhang, L.; Wu, S.; Wu, Y. *Food Chem.* **2003**, *80*, 283–290.
- (14) Haslam, E. *Phytochemistry* **2003**, *64*, 61–73.
- (15) Ozawa, T.; Kataoka, M.; Morikawa, K.; Negishi, O. *Biosci. Biotech. Biochem.* **1996**, *60*, 2023–2027.
- (16) Tanaka, T.; Betsumiya, Y.; Mine, C.; Kouno, I. *Chem. Commun.* **2000**, 1365–1366.
- (17) Tanaka, T.; Inoue, K.; Betsumiya, Y.; Mine, C.; Kouno, I. *J. Agric. Food Chem.* **2001**, *49*, 5785–5789.
- (18) Tanaka, T.; Mine, C.; Inoue, K.; Matsuda, M.; Kouno, I. *J. Agric. Food Chem.* **2002**, *50*, 2142–2148.
- (19) Tanaka, T.; Mine, C.; Kouno, I. *Tetrahedron* **2002**, *58*, 8851–8856.
- (20) Li, Y.; Tanaka, T.; Kouno, I. *Phytochemistry* **2007**, *68*, 1081–1088.
- (21) Kusano, R.; Tanaka, T.; Matsuo, Y.; Kouno, I. *Chem. Pharm. Bull.* **2007**, *55*, 1768–1772.
- (22) Tanaka, T.; Watarumi, S.; Matsuo, Y.; Kamei, M.; Kouno, I. *Tetrahedron* **2003**, *59*, 7939–7947.
- (23) Tanaka, T.; Matsuo, Y.; Kouno, I. *J. Agric. Food Chem.* **2005**, *53*, 7571–7578.

- (24) Matsuo, Y.; Tanaka, T.; Kouno, I. *Tetrahedron* **2006**, *62*, 4774–4783.
- (25) Matsuo, Y.; Tanaka, T.; Kouno, I. *Tetrahedron Lett.* **2009**, *50*, 1348–1351.
- (26) Tanaka, T.; Mine, C.; Watarumi, S.; Fujioka, T.; Mihashi, K.; Zhang, Y.-J.; Kouno, I. *J. Nat. Prod.* **2002**, *65*, 1582–1587.
- (27) Nonaka, G.; Kawahara, O.; Nishioka, I. *Chem. Pharm. Bull.* **1983**, *31*, 3906–3914.
- (28) Hashimoto, F.; Nonaka, G.; Nishioka, I. *Chem. Pharm. Bull.* **1988**, *36*, 1676–1684.

NP900618V